

Studies of Spin-Orbit Correlations with Longitudinally Polarized Target

Update of Experiment E12-07-107 (approved by PAC 32)

H. Avakian^{†*}, P.Bosted[†], A. Deur, V.D. Burkert, L.Elouadrhiri, A. Prokudin
Jefferson Lab, Newport News, VA 23606, USA

K. Griffioen[†]

College of William & Mary, VA 23187, USA

K. Hafidi[†], J. Arrington, L. El Fassi, D. F. Geesaman, R. J. Holt,
D. H. Potterveld, P. E. Reimer, P. Solvignon
Argonne National Lab, Argonne, IL 60439, USA

P. Rossi[†], E. De Sanctis, L. Hovsepyan, M. Mirazita, and S. Anefalos Pereira
INFN, Laboratori Nazionali di Frascati , Via E. Fermi, I-00044 Frascati, Italy

D. Crabb, L.C. Smith

UVA, Charlottesville, VA 22904, USA

M. Amarian, S. Bültmann, S. Kuhn

Old Dominion University, Norfolk, VA 23529, USA

F. Benmokhtar

University of Maryland, USA

Y. Prok

Christopher Newport University

D. Ireland, R. Kaiser, K. Livingston, G. Rosner, B. Seitz
Univ. of Glasgow, Glasgow G12 8QQ, UK

A. Danagoulian, H. Hakobyan

Yerevan State University, 1 Alex Manoogian, Yerevan, Armenia

M. Anselmino, A. Kotzinian, B. Parsamyan

Università di Torino and INFN, Sezione di Torino, Via P. Giuria 1, I-10125 Torino

P. Schweitzer, University of Connecticut, Storrs, CT 06269, USA

E. Di Salvo, Dipartimento di Fisica and INFN, Sezione di Genova, Via Dodecaneso, 33 I-16146 Genova, Italy

L. Gamberg, Penn State Berks, Reading, PA 19610, USA

G.R. Goldstein, Tufts University, Medford, MA 02155, USA

A CLAS collaboration proposal

[†] Co-spokesperson * Contact: Harut Avakian, JLab, Newport News VA 23606. Email: avakian@jlab.org

Abstract

We are proposing a comprehensive program to study transverse momentum dependence of valence quark transverse and longitudinal spin distributions through measurements of single-spin and double-spin azimuthal asymmetries in semi-inclusive electroproduction of pions using the upgraded JLab 11 GeV polarized electron beam and the CLAS12 detector with a longitudinally polarized proton and deuteron targets. Main objectives include studies of correlations of the transverse spin of quarks with their transverse momentum, leading to observable single spin asymmetries (SSA), and flavor decomposition of distributions of quarks aligned, q^+ , and anti-aligned, q^- , with proton spin as a function of both longitudinal, x , and transverse momentum of the quark, k_T . The measurement of the $\sin 2\phi$ azimuthal moment of the target spin-dependent part of the cross section, in particular will provide direct information on spin-orbit correlations by measuring the leading twist transverse momentum dependent (TMD) parton distribution related to the interference between states with different orbital momenta. The P_T dependence of the double spin asymmetry will provide additional information on the flavor and polarization dependence of transverse momentum dependence of helicity distributions of quarks, providing complimentary to SSA measurements access to spin-orbit correlations. The x, z, P_T and Q^2 dependences of the $\sin \phi$ to $\sin 2\phi$ moments will be studied to probe the underlying T-odd distribution and fragmentation functions as well as verify the hypothesis that the former is twist-3, and the later twist-2. The experiment will use the upgraded CLAS12 detector, 11 GeV highly polarized electron beam, and longitudinally polarized solid ammonia targets (NH_3 and ND_3). Large acceptance of CLAS12, would allow simultaneous detection of the scattered electrons and leading hadrons from the hadronization of the struck quark, providing information on its flavor and transverse momentum. We request 30 days of running on NH_3 and 50 days of running on ND_3 (or possibly ^6LiD or HD), including about 20% overhead for target anneals, polarization reversal, and auxiliary measurements.

| N/q | U | L | T |
|-----|----------------|----------------|-------------------------------|
| U | \mathbf{f}_1 | | h_1^\perp |
| L | | \mathbf{g}_1 | h_{1L}^\perp |
| T | f_{1T}^\perp | g_{1T} | \mathbf{h}_1 h_{1T}^\perp |

Table 1: Leading-twist transverse momentum-dependent distribution functions. U , L , and T stand for transitions of unpolarized, longitudinally polarized, and transversely polarized nucleons (rows) to corresponding quarks (columns).

1 Introduction

In recent years, semi-inclusive deep inelastic scattering (SIDIS) has emerged as a powerful tool to probe nucleon structure through transverse single spin asymmetries (SSAs) [1, 2, 3, 4, 5, 6, 7, 8]. In contrast to inclusive deep inelastic lepton-nucleon scattering where transverse momentum is integrated out, these processes are sensitive to transverse momentum scales on the order of the intrinsic quark momentum $P_T \sim k_\perp$. Azimuthal distributions of final state particles in semi-inclusive deep inelastic scattering provide access to the orbital motion of quarks and play an important role in the study of transverse momentum distributions (TMDs) of quarks in the nucleon.

Significant progress has been recently made in understanding the role of partonic initial and final state interactions [9, 10, 11]. The interaction between the active parton in the hadron and the spectators leads to gauge-invariant transverse momentum dependent (TMD) parton distributions [9, 10, 11, 12, 13, 14]. Furthermore, QCD factorization for semi-inclusive deep inelastic scattering at low transverse momentum in the current-fragmentation region has been established in Refs. [15, 16]. This new framework provides a rigorous basis to study the TMD parton distributions from SIDIS data using different spin-dependent and spin-independent observables. TMD distributions (see Table 1) describe different spin-spin and spin-orbit correlations in the momentum space [17, 18, 19, 20]. Knowledge of TMDs is also crucial for understanding phenomena in high energy hadronic scattering processes, such as, the single transverse spin asymmetries [9, 21, 10, 11, 12, 22].

The diagonal elements of the table are the momentum, longitudinal and transverse spin distributions of partons, and represent parton distribution functions related to the square of the leading-twist, light-cone wave functions. The off-diagonal TMD distributions arise from interference between amplitudes with left- and right-handed polarization states, and only exist because of chiral symmetry breaking in the nucleon wave function in QCD. Their study therefore provides a new avenue for probing the chiral nature of the partonic structure of hadrons. The universality of the TMD correlation functions has been proven, resulting in a sign change for two T -odd TMD distributions between Drell-Yan and DIS [10, 16], an exciting prediction that has to be confirmed by future experiments.

Measurements of transverse momentum P_T of final state hadrons in SIDIS with longitudinally polarized leptons and nucleons provide access to leading twist helicity $g_{1L}(x, k_T)$ TMD. Recent measurements of multiplicities and double spin asymmetries as a function of the final transverse momentum of pions in SIDIS at JLab [23, 24] suggest that transverse momentum distributions may depend on the polarization of quarks and possibly also on their flavor. Calculations of transverse momentum dependence of TMDs in different models [25, 26, 27, 28] and on lattice [29, 30] indicate that dependence of transverse momentum distributions on the quark polarization and flavor may be very significant. Orbital momentum of quarks changes significantly the helicity distribution of quarks in the valence quark region, in particular the distributions of quarks anti-aligned, with proton spin [31]. Simple model calculations also indicate that quark distributions aligned, q^+ , and anti-aligned, q^- , with proton spin will have also very different transverse momentum distributions [32]. That may lead to observable effects in transverse momentum, P_T , dependences of double-spin longitudinal asymmetries [26]. The latest results on TMDs from the Lattice QCD calculations [29, 33, 30], indicate that spin-orbit correlations could change the transverse momentum distributions of partons. Measurements of transverse momentum dependence of helicity distributions will be also important for interpretation of ongoing studies at different facilities worldwide of gluon polarization using high P_T hadrons [34, 35, 36, 37].

Measurement of the azimuthal modulation of the cross section in double polarized SIDIS, in addition provides access to the “worm gear” h_{1L}^\perp TMD, describing transversely polarized quarks in the longitudinally polarized nucleon. The h_{1L}^\perp distribution function has been studied in various QCD inspired models [38, 39, 27, 40, 41, 42], including large- x [43] and large N_c [44] limits of QCD. Calculations for $h_{1L}^\perp(x, k_T)$ have recently been performed in the perturbative limit [45], and first measurements have been performed using lattice methods [29]. A measurably large asymmetry has been predicted only at large x ($x > 0.2$), a region well-covered by JLab.

PAC32 approved Experiment E12-07-107, in which we proposed 80 days of measurements with polarized electron beam on a polarized hydrogen and deuterium target together with CLAS12 at its maximum luminosity. This experiment will take full advantage of the unique combination of wide kinematic coverage, high beam intensity (luminosity), high energy, high polarization, and advanced detection capabilities to study the transverse momentum and spin correlations in double-polarized semi-inclusive processes both in the target and current fragmentation regions.

2 Scientific Case and Recent Developments

The SIDIS cross section at leading twist has eight contributions related to different combinations of the polarization state of the incoming lepton and the target nucleon [46, 47, 15, 18]. The lepton-hadron cross section can then be parametrized as [18]

$$\begin{aligned}
\frac{d\sigma}{dx dy dz d\phi_S d\phi_h dP_{h\perp}^2} &= \frac{\alpha^2}{xQ^2} \frac{y}{2(1-\varepsilon)} \\
&\times \left\{ F_{UU,T} + \varepsilon \cos(2\phi_h) F_{UU}^{\cos 2\phi_h} + S_L \varepsilon \sin(2\phi_h) F_{UL}^{\sin 2\phi_h} \right. \\
&\quad + S_L \lambda_e \sqrt{1-\varepsilon^2} F_{LL} + |\mathbf{S}_T| \left[\sin(\phi_h - \phi_S) F_{UT,T}^{\sin(\phi_h - \phi_S)} \right. \\
&\quad \left. \left. + \varepsilon \sin(\phi_h + \phi_S) F_{UT}^{\sin(\phi_h + \phi_S)} + \varepsilon \sin(3\phi_h - \phi_S) F_{UT}^{\sin(3\phi_h - \phi_S)} \right] \right. \\
&\quad \left. + |\mathbf{S}_T| \lambda_e \left[\sqrt{1-\varepsilon^2} \cos(\phi_h - \phi_S) F_{LT}^{\cos(\phi_h - \phi_S)} \right] \right\}, \tag{1}
\end{aligned}$$

where α is the fine structure constant and ε the ratio of longitudinal and transverse photon flux,

$$\varepsilon = \frac{1-y}{1-y+y^2/2}. \tag{2}$$

The kinematic variables x , y are defined as: $x = Q^2/2(P_1q)$, and $y = (P_1q)/(P_1k_1)$. The variable $q = k_1 - k_2$ is the momentum of the virtual photon, $Q^2 = -q^2$, ϕ_h is the azimuthal angle between the scattering plane formed by the initial and final momenta of the electron and the production plane formed by the transverse momentum of the observed hadron and the virtual photon, and ϕ_S is the azimuthal angle of the transverse spin in the scattering plane [48]. The subscripts in F_{UL} , F_{LL} , etc., specify the beam (first index) and target(second index) polarizations, longitudinal (L), transverse (T), and unpolarized (U). S_L and S_T are longitudinal and transverse components of the target polarization with respect to the direction of the virtual photon.

Structure functions factorize into TMD parton distributions and fragmentation functions, and hard parts [15]

$$\begin{aligned}
\sigma_{UU} \propto F_{UU} \propto & f_1(x, k_\perp) D_1(z_h, p_\perp) H_{UU}(Q^2) \\
\sigma_{LL} \propto F_{LL} \propto & g_{1L}(x, k_\perp) D_1(z_h, p_\perp) H_{LL}(Q^2) \\
\sigma_{UL} \propto F_{UL} \propto & h_{1L}^\perp(x, k_\perp) H_1^\perp(z_h, p_\perp) H_{UL}(Q^2), \tag{3}
\end{aligned}$$

where $z = (P_1P_h)/(P_1q)$, k_\perp and p_\perp are quark transverse momenta before and after scattering, and P_1 and P_h are the four momenta of the initial nucleon and the observed final-state hadron respectively.

The unpolarized D_1 and polarized H_1^\perp [49] fragmentation functions depend in general on the transverse momentum of the fragmenting quark. The different hard factors (H_{UU} , H_{LL} , etc.), which are calculable in pQCD, in the SIDIS cross section are similar at one-loop order [15] and may cancel to a large extent in asymmetry observables.

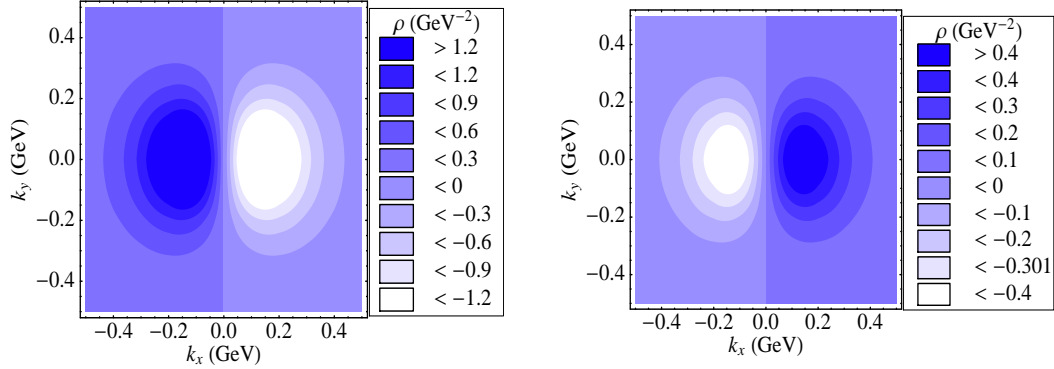


Figure 1: Quark densities in the \mathbf{k}_T plane for transversely polarized quarks in a longitudinally polarized proton for up (left panel) and down (right panel) quark.

2.1 Transversely polarized quarks in the longitudinally polarized nucleon

Spin-orbit correlations are accessible in SIDIS with longitudinally polarized target in measurements of double and single-spin asymmetries. For a longitudinally polarized target the only azimuthal asymmetry arising in leading order is the $\sin 2\phi$ moment,

$$F_{UL}^{\sin 2\phi_h} = \mathcal{F} \left[- \frac{2(\hat{\mathbf{h}} \cdot \mathbf{p}_T)(\hat{\mathbf{h}} \cdot \mathbf{k}_T) - \mathbf{p}_T \cdot \mathbf{k}_T}{M_N M_h} h_{1L}^\perp H_1^\perp \right], \quad (4)$$

where $\hat{\mathbf{h}} \equiv \mathbf{P}_{h\perp}/P_{h\perp}$ and $\mathcal{F}[fD] = x \sum_a e_a^2 \int d\mathbf{k}_T d\mathbf{p}_T \delta^{(2)}(\mathbf{k}_T - \mathbf{p}_T - \mathbf{P}_{h\perp}/z) f^a(x, k_T^2) D^a(z, p_T^2)$, and e_a is the electric charge of a quark of flavor a .

The distribution function giving rise to SSA, h_{1L}^\perp , is related to the real part of the interference of wave functions for different orbital momentum states. It involves helicity flip of the quarks but is diagonal in the nucleon helicity. One of the characteristic features of h_{1L}^\perp is that it has no analog in the spin densities related to the GPDs in the impact parameter space [50, 51]. The results in the light-cone quark model [27] for the densities with transversely polarized quarks in a longitudinally polarized proton shown in Fig. 1 are in good agreement with recent lattice calculation[29, 33]. For the density related to h_{1L}^\perp , they predict shifts of similar magnitude of $\langle \mathbf{k}_x^u \rangle = -60(5)$ MeV, and $\langle \mathbf{k}_x^d \rangle = 15(5)$ MeV.

The physics of σ_{UL} , which involves the Collins fragmentation function H_1^\perp and “worm gear” distribution function h_{1L}^\perp , was first discussed by Kotzinian and Mulders in 1996 [47, 46, 52]. The same distribution function is also accessible in double-polarized Drell-Yan production, where it gives rise to the $\cos 2\phi$ and $\sin 2\phi$ azimuthal moment in the cross section [53, 54].

During the last few years, first results on longitudinal target SSAs have become available from HERMES, COMPASS and CLAS [1, 55, 56, 24, 7]. Measurement of the

$\sin 2\phi$ moment of σ_{UL} in the relatively low x -range by HERMES [1] and COMPASS [7] are consistent with zero. A measurably large asymmetry has been predicted only at large x ($x > 0.2$), a region well-covered by JLab [57, 38, 39, 40, 41, 58]. The data from CLAS at 6 GeV indicate large azimuthal moments both for $\sin \phi$ and $\sin 2\phi$ [24]. The phenomenological studies of the $\sin 2\phi_h$ asymmetry in the longitudinally polarized SIDIS process [1, 59, 24] have been performed in [60, 61, 39] and recently in [42, 41], showing that the asymmetry is around several per cent.

The measurement of transverse spin dependent distributions is complicated by the presence of an additional polarized fragmentation function. Significant asymmetry was measured recently by Belle [62, 63, 64], indicating that the Collins function is indeed large.

2.2 Flavor and transverse momentum dependence of helicity distributions

Measurements of transverse momenta of final state hadrons in SIDIS with longitudinally polarized targets will provide complementary to transverse target information, probing the longitudinal nucleon structure beyond the collinear approximation. The P_\perp -dependence of the double-spin asymmetry, measured for different bins in z and x will provide a test of the factorization hypothesis and probe the transition from the non-perturbative to perturbative description. At large P_T ($\Lambda_{QCD} \ll P_T \ll Q$) the asymmetry is expected to be independent of P_\perp [15].

There are indications from different model calculations [26, 28] and lattice [30] that the double-spin asymmetry at small P_T may have some dependence on P_T making it an attractive observable to study the helicity dependence of k_T -distributions. Latest CLAS measurements indicate [24] the double-spin asymmetry tends to increase for π^- and decrease for π^+ . A possible interpretation of the P_T -dependence of the double spin asymmetry may involve different widths of transverse momentum distributions of quarks with different flavor and polarization [26] resulting from a different orbital structure of quarks polarized in the direction of the proton spin and opposite to it [65, 66]. This interpretation may demand a different width for d -quarks than for u -quarks, consistent with observation from lattice QCD studies of a different spread in transverse distances for d -quarks compared to u -quarks [67].

Detailed measurements of A_{LL} and its $\cos \phi$ moment as a function of P_T in different bins in x, z, Q^2 combined with measurements of azimuthal moments of the unpolarized cross section proposed for CLAS12 will allow study of the flavor dependence of transverse momentum distributions. The P_\perp -dependence of the double-spin asymmetry, measured for different bins in z and x will also provide a test of the factorization hypothesis and probe the transition from the non-perturbative to perturbative description. At large P_T ($\Lambda_{QCD} \ll P_T \ll Q$) the asymmetry is expected to be independent of P_\perp [15].

To do a P_T -dependent flavor decomposition and extract the transverse momen-

tum dependent helicity distributions $q^+(x, k_T), q^-(x, k_T)$, double spin asymmetries have to be extracted in bins in P_T . The P_T -dependent cross section is given by[26]:

$$\sigma_{LL} = \frac{\pi}{xy^2} \left[y(2-y) \right] \Sigma_q e_q^2 \int d^2\mathbf{k}_\perp g_{1L}^q(x, \mathbf{k}_\perp) D_q^h(z, \mathbf{P}_{hT} - z\mathbf{k}_\perp), \quad (5)$$

$$\sigma_0 = \frac{\pi}{xy^2} \left[1 + (1-y)^2 \right] \Sigma_q e_q^2 \int d^2\mathbf{k}_\perp f_1^q(x, \mathbf{k}_\perp) D_q^h(z, \mathbf{P}_{hT} - z\mathbf{k}_\perp). \quad (6)$$

In order to extract TMDs, it is therefore advantageous to project the differential cross section onto Fourier modes [68]. At leading twist and tree-level, the weighted integral of cross section can be related to a product of TMDs and fragmentation functions in Fourier space.

$$\begin{aligned} & \int_0^{2\pi} \frac{d\phi_S}{2\pi} \int_0^{2\pi} d\phi_h \int_0^\infty d|\mathbf{P}_{h\perp}| |\mathbf{P}_{h\perp}| J_0(|\mathbf{P}_{h\perp}||\mathbf{b}_T|) \left[\frac{d\sigma}{dx_B dy d\phi_S dz_h d\phi_h |\mathbf{P}_{h\perp}| d|\mathbf{P}_{h\perp}|} \right] \\ &= \frac{\alpha^2}{yQ^2} \frac{y^2}{(1-\varepsilon)} \left(1 + \frac{\gamma^2}{2x_B} \right) \sum_a e_a^2 \left\{ \tilde{f}_1^a(x, z^2 \mathbf{b}_T^2) + S_{\parallel} \lambda_e \sqrt{1-\varepsilon^2} \tilde{g}_1^a(x, z^2 \mathbf{b}_T^2) \right\} \tilde{D}_1^a(z, \mathbf{b}_T^2), \end{aligned}$$

where Fourier transform of a generic TMD f (or a generic fragmentation function D) is defined as

$$\tilde{f}(x, \mathbf{b}_T^2) \equiv \int d^2\mathbf{k}_T e^{i\mathbf{b}_T \cdot \mathbf{k}_T} f(x, \mathbf{k}_T^2) = 2\pi \int d|\mathbf{k}_T| |\mathbf{k}_T| J_0(|\mathbf{b}_T||\mathbf{k}_T|) f^a(x, \mathbf{k}_T^2), \quad (7)$$

where J_0 is a Bessel function. The formalism in \mathbf{b}_T -space avoids convolutions, making it easier to perform a model independent analysis. The fundamental objects in this formalism are the (derivatives of) Fourier transformed TMDs $\tilde{f}_1, \tilde{g}_1, \tilde{h}_{1L}^{\perp(1)}$ ¹ and fragmentation functions $\tilde{D}_1^{(0)}, \tilde{H}_1^{\perp(1)}$. Theoretically, these $|\mathbf{b}_T|$ -dependent distributions contain the same information as their conventional, momentum dependent counterparts. In practice, however, only a limited range in $|\mathbf{b}_T|$ is accessible with sufficient accuracy from experiments. Thus, to carry out the Fourier transformation back to conventional TMDs, model assumptions must be made in order to supplement information over the whole range of $|\mathbf{b}_T|$.

The $|\mathbf{b}_T|$ -dependent distributions are also the objects that appear in the evolution equations that describe the scale dependence beyond tree level, see, e.g., Ref. [69]. Lattice calculations of TMDs are performed in b -space rather than momentum space as well [29, 30]. This suggests that it is the $|\mathbf{b}_T|$ -dependent quantities that are most suitable for a model independent analysis and comparison with lattice data.

Main questions to address, when applying this procedure to CLAS12 data, are the limited range in hadron transverse momenta and the low Q^2 , as Fourier-transformed quantities receive (through the Fourier integral) contributions from the entire range

¹1 indicates first derivative over \mathbf{b}_T

of P_T , while the whole factorization formalism requires $P_T \ll Q$. The studies of effects of the cut on the maximum value of P_T are in progress.

The unpolarized contribution from f_1 can be isolated from that of g_1 by averaging over the helicity of the electron λ_e . The above transformation depends on the external parameter $\mathcal{B}_T \equiv |\mathbf{b}_T|$. Choosing different values of this parameter allows us to scan the transverse momentum dependence of the distributions in Fourier space.

Measured single and double spin asymmetries for all pions in a large range of kinematic variables (x_B , Q^2 , z , P_\perp , and ϕ) combined with measurements with unpolarized targets will provide detailed information on the flavor and polarization dependence of the transverse momentum distributions of quarks in the valence region, and in particular, on the x_B and k_T dependence of the leading TMD parton distribution functions of u and d quarks.

3 Technical Progress Towards Realizing the Experiment

The proposed experiment will use the upgraded CLAS12 spectrometer in its standard configuration. We will run at the maximum magnetic field. Running conditions will be similar to already approved CLAS12 proposal for inclusive DIS studies with CLAS12 [70].

The major non-standard item required for successful execution of this program is the polarized target. The work has begun on the detailed design of all target components, in particular the in-beam cryostat and vacuum vessel. The design of the central Silicon Vertex Tracker for CLAS12 is now fully consistent with the required space to insert the polarized target into its center. Initial development work has also begun on the target insert and NMR system; several major components and measuring instruments have already been acquired. The total project, which also receives strong support from the JLab target group, is on track to be completed within 3 years, making the polarized target available as soon as the experimental program with CLAS12 can begin. The first-level trigger will consist of a coincidence between the high-threshold Cerenkov counter and a signal above threshold (corresponding to at least 1 GeV deposited) in the electromagnetic calorimeter in the same sector. This trigger will be highly specific for high-energy electrons, with little contamination from pions and other particles. The total event rate in the DIS region for this experiment is expected to be around 2000 Hz above $Q^2 = 1 \text{ GeV}^2$. Estimates of the total trigger rate are around 20 kHz. A data acquisition rate of 10 kHz has already been achieved with today's technology for the present CLAS DAQ, so that the required data acquisition rate for this experiment is a rather modest extrapolation.

At PAC34, a series of SIDIS experiments (Proposals E12-09-007, 008, 009) were approved for both unpolarized and longitudinally polarized target. All of these proposal require a RICH detector to separate Kaons from pions and protons. Work on the

design of such a RICH detector has begun, and first benchmark results have been presented at CLAS12 workshops. That will extend all proposed measurements, allowing separation of all three charge states of pions and kaons and studies of fragmentation process of hadrons.

4 The Beam Request and Expected Results

We will run with a beam of about 10 nA on a 3 cm long ammonia target, resulting in a luminosity of $10^{35}/\text{cm}^2\text{s}$. The beam will be rastered over the diameter of the polarized target (about 3 cm) to minimize the dose density (we will need at most one anneal every other day under these conditions). We assume a beam polarization of 0.85, which has been routinely achieved in recent experiments running at Jefferson Lab. The beam helicity will be flipped in a pseudo-random pattern every 33 ms. We will use the standard Hall B beam devices to monitor and stabilize the beam intensity and position. In particular, we will reduce any helicity-correlated beam asymmetries to less than 10^{-3} .

The data will consist of the number of counts for beam helicity anti-parallel (N^+) and parallel (N^-) to the longitudinal target polarization, each normalized to the dead-time corrected integrated beam charge and form the ratio $A_{||}^{raw} = (N^+ - N^-)/(N^+ + N^-)$. This ratio has to be divided by the product of beam and target polarization and the dilution factor (the fraction of counts coming from the polarized nuclei in the target to the total).

The dilution factor can be calculated from a detailed model of the target content and a parametrization of the world data on unpolarized structure function for nucleons and nuclei (^{15}N , ^4He , and C and Al foils) in the target, including radiative effects. The beam (P_B) and target (P_T) polarization will be independently measured using Möller scattering and NMR, respectively.

The expected number of counts and corresponding statistical errors in the following sections are based on a full simulation of inclusive and semi-inclusive inelastic scattering with the CLAS12 acceptance folded in. Events were generated with the clas12DIS generator [71]. This generator is basically an implementation of the LUND Monte Carlo package called PEPSI (Polarized Electron-Proton Scattering Interactions) [72]. It is based on polarized and unpolarized parton distribution functions and the LUND string model for hadronization, and has been tested successfully against several low- Q^2 experiments with 5.7 GeV beam at Jefferson Lab.

A fast Monte Carlo simulation program has been used to define the acceptance and resolution of the CLAS12 detector with all of the standard (base) equipment in place.

Table 2: Uncertainties for asymmetry measurements.

| Item | A_1^p | $A_{UL}^{\sin \phi}$ | $A_{UL}^{\sin 2\phi}$ |
|--|---------|----------------------|-----------------------|
| beam x target polarization | 2% | - | - |
| target polarization | - | 3% | 3% |
| depolarization and R | 4% | - | - |
| dilution factor | 3% | 3% | 3% |
| radiative corrections | 3% | 3% | 3% |
| fitting procedure | - | 4% | 5% |
| transverse (to γ^*) spin effects | 3% | 3% | -% |

4.1 Statistical and systematic errors

The main sources of systematic errors include the beam and target polarizations, dilution factor the longitudinal to transverse photo absorption cross section ratio, $R(x, Q^2)^2$. The main sources of systematic errors in measurements of single and double spin asymmetries are listed in the Table 2. These errors are all scale errors, so are proportional to the size of the measured asymmetry. The total uncertainty is expected to be less than 10% of the measured SSA. Most of the contributions to systematic error of measured asymmetries will come from uncertainties of unpolarized structure functions and also attenuation of hadrons in nuclear environment, which are a subject of a separate study (PAC-30 proposal on nuclei)

For the $\sin 2\phi$ SSA, statistical uncertainties are expected to dominate the total uncertainty. Studies of other sources of systematics, related to physics background, including target fragmentation, semi-exclusive processes, exclusive vector meson contributions and higher twist require the data of this measurement.

We base our predicted statistical errors in the following sections on the assumption of running 30 days on NH_3 and 50 days on ND_3 . The number of days was chosen to achieve a statistical error that is not significantly larger than the systematical error at the highest x and P_T points. More days on deuterium than the proton ensures that both have the same statistical error at large P_T and optimizes the error on extracted quantities like $h_{1L}^{\perp u,d}$ and $\Delta d_v/d_v$.

4.2 Results

The proposed experiment will simultaneously collect data on $\vec{p}, \vec{d}(\vec{e}, e'\pi^{+,0,-})$. Projected error bars for the h_{1L}^{\perp} TMD parton distribution are shown in Fig. 2. Estimates are performed assuming the so-called ‘‘Lorentz-invariance relations’’ that connect h_{1L}^{\perp} with h_1 [47]. This measurement will check out experimentally to which extent such relations actually hold [74, 17].

²A subject of a dedicated experiment E12-06-112 in Hall-C

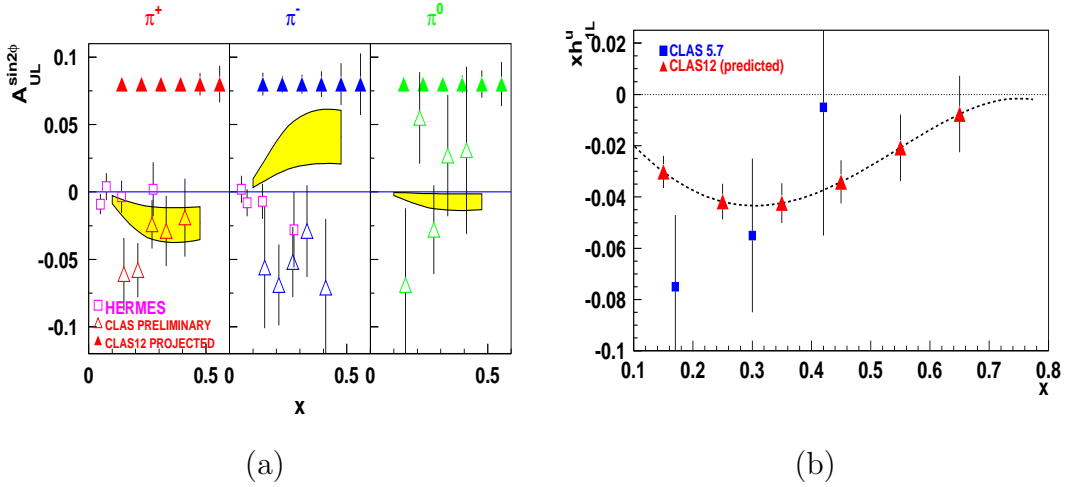


Figure 2: (Left) The projected x -dependence of the target SSA at 11 GeV. The triangles illustrate the expected statistical accuracy. The open squares and triangles show the existing measurement of the Mulders TMD from HERMES and the preliminary results from CLAS 5.7 GeV EG1 data sets, respectively. The curves are calculated using Ref. [73]. (Right) Projection for the Mulders distribution function for the u -quark from the π^+ SSA from CLAS12 (predicted) compared with the CLAS EG1 data set at 5.7 GeV.

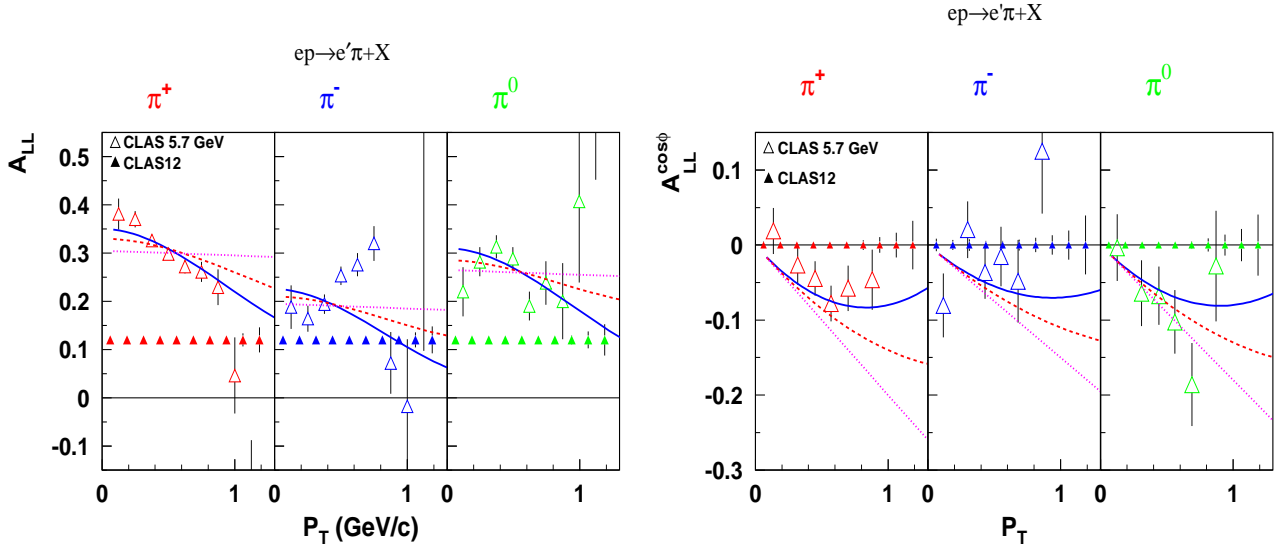


Figure 3: The double spin asymmetry A_{LL} (left) and its $\cos\phi$ moment (right) for the NH_3 -target as a function of the transverse momentum of hadrons, P_T , averaged in the $0.4 < z < 0.7$ range. Curves are calculated using different k_T widths for helicity distributions [26].

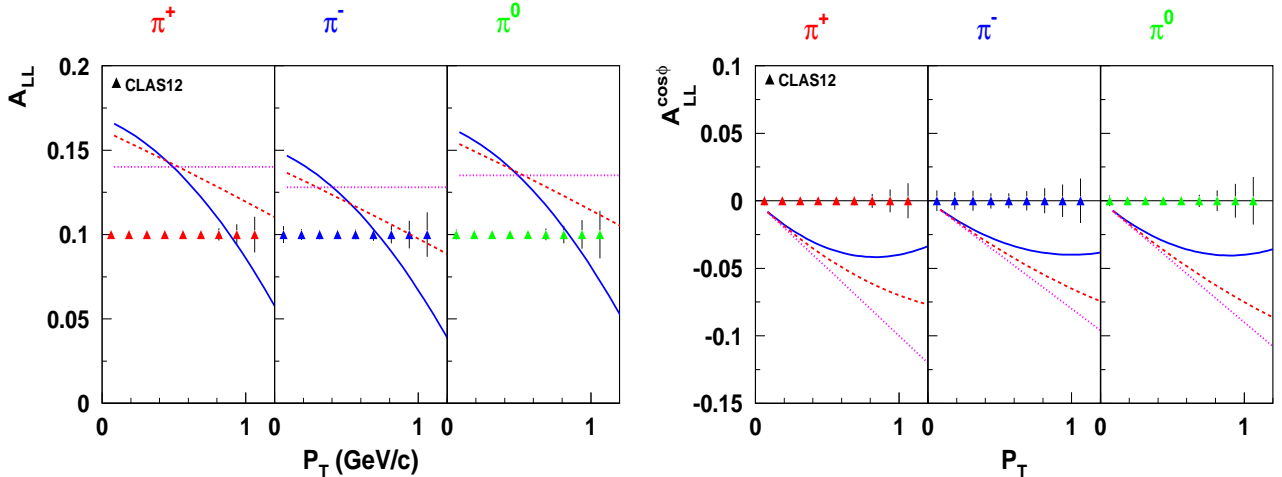


Figure 4: The double spin asymmetry A_{LL} (left) and its $\cos\phi$ moment (right) for the ND_3 -target as a function of the transverse momentum of hadrons, P_T , averaged in the $0.4 < z < 0.7$ range. Curves are calculated using different k_T widths for helicity distributions [26].

The combined analysis of the future CLAS12 data on $\langle \sin 2\phi \rangle$ and of the previous HERMES and COMPASS [1, 55, 7] measurements in the high- Q^2 domain (where higher-twist effects are less significant) will provide information on the “worm gear” function, shedding light on the correlations between transverse spin and transverse momenta of quarks. Significantly increasing the kinematic coverage at large Q^2 and P_T , CLAS12 (see Fig. 2) will map the quark TMDs in the valence region allowing study of the transition from a non-perturbative description at small P_T to a perturbative description at large P_T . Complementary, to our measurements with proton and deuteron targets, information will come also from approved polarized ^3He target experiment in Hall-A [75].

A very large data set (in particular at lower x) allows us to further subdivide the data into bins in p_T and z . Once in hand, these data will be combined with existing SIDIS data from HERMES, COMPASS and RHIC for a full NLO analysis. From this analysis, we will extract the polarized PDFs for each quark and antiquark flavor in the region $0.1 \leq x \leq 0.8$. Projections for the resulting P_T -dependence of the double spin asymmetries for all three pions are shown in Fig. 3 and Fig. 4 for NH_3 and ND_3 targets respectively. These measurements using unfolding of Eqs.5-6 would allow access the k_T -distributions of u and d -quarks aligned and anti-aligned with the spin of the nucleon. Integrated over the transverse momentum the data will be also used to extract the k_T -integrated standard PDFs.

| Time | Activity |
|--|--|
| 3 days | Commissioning: Beam raster set up, trigger optimization, low energy calibration runs |
| 30 days | Production data taking on NH_3 |
| 50 days | Production data taking on ND_3 |
| 3 days (1 1/2 hours every other day) | Target anneals and/or target changes |
| 10 days (intermittent with production data) | Calibration runs on ^{12}C and empty target |
| 5 days | Production runs on ^{15}N |
| 2 day (1 hour every other day – concurrent with anneals) | Möller polarimeter runs |

Table 3: Requested beam time broken down by activity.

4.3 Summary and Request

Understanding of spin-orbit correlations, together with independent measurements related to the spin and orbital angular momentum of the quarks, will help to construct a more complete picture of the nucleon in terms of elementary quarks and gluons going beyond the simple collinear partonic representation. The proposed set of measurements on longitudinally polarized proton and deuteron targets will yield a comprehensive set of single and double spin asymmetries providing access to corresponding distribution and fragmentation functions in a wide range of x , Q^2 , z and P_T . Our data, combined with the data from HERMES, COMPASS and BELLE, will allow us to extract leading twist TMD parton distributions $g_1(x, k_T)$ and $h_{1L}(x, k_T)$ and improve considerably our knowledge of higher twist contributions to different azimuthal moments of spin dependent cross section.

To achieve this goal, we request a total of 103 days of beam time with an 11 GeV, 10 nA highly polarized electron beam in Hall B. The breakdown of this beam time is shown in Table 3. The number of days requested was chosen to optimize the impact of our data and to make the systematic and statistical errors roughly equal for the highest x data points.

We want to conclude by noting that while this experiment requires a substantial commitment of beam time (103 days total), most of the time we will simultaneously take data with already approved experiment to study the inclusive DIS [70]. In addition, the proposed experiment will yield data on single (target and beam) spin asymmetries in SIDIS which can provide constraints on the higher-twist nucleon structure functions and provide complementary to transverse target information on spin-orbit correlations (the LOI submitted to PAC-30 [76]).

References

- [1] HERMES, A. Airapetian et al., Phys. Rev. Lett. 84 (2000) 4047, hep-ex/9910062.
- [2] HERMES, A. Airapetian et al., Phys. Rev. Lett. 94 (2005) 012002, hep-ex/0408013.
- [3] COMPASS, V.Y. Alexakhin et al., Phys. Rev. Lett. 94 (2005) 202002, hep-ex/0503002.
- [4] COMPASS, E.S. Ageev et al., Nucl. Phys. B765 (2007) 31, hep-ex/0610068.
- [5] HERMES, A. Airapetian et al., Phys. Lett. B693 (2010) 11, 1006.4221.
- [6] The COMPASS, M.G. Alekseev et al., Phys. Lett. B692 (2010) 240, 1005.5609.
- [7] M.G. Alekseev et al., Eur. Phys. J. C70 (2010) 39, 1007.1562.
- [8] X. Qian et al., (2011), nucl-ex/1106.0363.
- [9] S.J. Brodsky, D.S. Hwang and I. Schmidt, Phys. Lett. B530 (2002) 99, hep-ph/0201296.
- [10] J.C. Collins, Phys. Lett. B536 (2002) 43, hep-ph/0204004.
- [11] X. Ji and F. Yuan, Phys. Lett. B543 (2002) 66, hep-ph/0206057.
- [12] A.V. Belitsky, X. Ji and F. Yuan, Nucl. Phys. B656 (2003) 165, hep-ph/0208038.
- [13] D. Boer, S.J. Brodsky and D.S. Hwang, Phys. Rev. D67 (2003) 054003, hep-ph/0211110.
- [14] D. Boer, P.J. Mulders and F. Pijlman, Nucl. Phys. B667 (2003) 201, hep-ph/0303034.
- [15] X. Ji, J. Ma and F. Yuan, Phys. Rev. D71 (2005) 034005, hep-ph/0404183.
- [16] J.C. Collins and A. Metz, Phys. Rev. Lett. 93 (2004) 252001, hep-ph/0408249.
- [17] K. Goeke, A. Metz and M. Schlegel, Phys. Lett. B618 (2005) 90, hep-ph/0504130.
- [18] A. Bacchetta et al., JHEP 02 (2007) 093, hep-ph/0611265.
- [19] S. Meissner, A. Metz and K. Goeke, Phys. Rev. D76 (2007) 034002, hep-ph/0703176.
- [20] C. Lorce and B. Pasquini, (2011), 1104.5651.

- [21] S.J. Brodsky, D.S. Hwang and I. Schmidt, Nucl. Phys. B642 (2002) 344, hep-ph/0206259.
- [22] Z.B. Kang and J.W. Qiu, Phys. Rev. Lett. 103 (2009) 172001, 0903.3629.
- [23] H. Mkrtchyan et al., Phys. Lett. B665 (2008) 20, hep-ph/0709.3020.
- [24] The CLAS, H. Avakian et al., Phys. Rev. Lett. 105 (2010) 262002, hep-ex/1003.4549.
- [25] Z. Lu and B.Q. Ma, Nucl. Phys. A741 (2004) 200, hep-ph/0406171.
- [26] M. Anselmino et al., Phys. Rev. D74 (2006) 074015, hep-ph/0608048.
- [27] B. Pasquini, S. Cazzaniga and S. Boffi, Phys. Rev. D78 (2008) 034025, hep-ph/0806.2298.
- [28] C. Bourrely, F. Buccella and J. Soffer, (2010), 1008.5322.
- [29] P. Hagler et al., Europhys. Lett. 88 (2009) 61001, hep-lat/0908.1283.
- [30] B.U. Musch et al., (2010), 1011.1213.
- [31] H. Avakian et al., Phys. Rev. Lett. 99 (2007) 082001, hep-ph/0705.1553.
- [32] R. Jakob, P.J. Mulders and J. Rodrigues, (1997), hep-ph/9707340.
- [33] B.U. Musch, (2009), 0907.2381.
- [34] HERMES, A. Airapetian et al., Phys. Rev. Lett. 84 (2000) 2584, hep-ex/9907020.
- [35] Spin Muon (SMC), B. Adeva et al., Phys. Rev. D70 (2004) 012002, hep-ex/0402010.
- [36] COMPASS, E.S. Ageev et al., Phys. Lett. B633 (2006) 25, hep-ex/0511028.
- [37] PHENIX, A. Adare, (2007), arXiv:0704.3599 [hep-ex].
- [38] L.P. Gamberg, G.R. Goldstein and M. Schlegel, Phys. Rev. D77 (2008) 094016, hep-ph/0708.0324.
- [39] H. Avakian et al., Phys. Rev. D77 (2008) 014023, hep-ph/0709.3253.
- [40] A.V. Efremov et al., Phys. Rev. D80 (2009) 014021, hep-ph/0903.3490.
- [41] S. Boffi et al., Phys. Rev. D79 (2009) 094012, hep-ph/0903.1271.
- [42] J. Zhu and B.Q. Ma, Phys. Lett. B696 (2011) 246, 1104.4564.

- [43] S.J. Brodsky and F. Yuan, Phys. Rev. D74 (2006) 094018, hep-ph/0610236.
- [44] P.V. Pobylitsa, hep-ph/0301236 (2003), hep-ph/0301236.
- [45] J. Zhou, F. Yuan and Z.T. Liang, Phys. Rev. D81 (2010) 054008, hep-ph/0909.2238.
- [46] A. Kotzinian, Nucl. Phys. B441 (1995) 234, hep-ph/9412283.
- [47] P.J. Mulders and R.D. Tangerman, Nucl. Phys. B461 (1996) 197, hep-ph/9510301.
- [48] A. Bacchetta et al., Phys. Rev. D70 (2004) 117504, hep-ph/0410050.
- [49] J.C. Collins, Nucl. Phys. B396 (1993) 161, hep-ph/9208213.
- [50] M. Diehl and P. Hagler, Eur. Phys. J. C44 (2005) 87, hep-ph/0504175.
- [51] B. Pasquini and S. Boffi, Phys. Lett. B653 (2007) 23, 0705.4345.
- [52] A.M. Kotzinian and P.J. Mulders, Phys. Rev. D54 (1996) 1229, hep-ph/9511420.
- [53] R.D. Tangerman and P.J. Mulders, Phys. Rev. D51 (1995) 3357, hep-ph/9403227.
- [54] Z. Lu, B.Q. Ma and J. She, (2011), 1104.5410.
- [55] HERMES, A. Airapetian et al., Phys. Rev. D64 (2001) 097101, hep-ex/0104005.
- [56] HERMES, A. Airapetian et al., Phys. Lett. B622 (2005) 14, hep-ex/0505042.
- [57] A.V. Efremov, K. Goeke and P. Schweitzer, Phys. Rev. D67 (2003) 114014, hep-ph/0208124.
- [58] J. Zhu and B.Q. Ma, (2011), 1104.5545.
- [59] HERMES, A. Airapetian et al., Phys. Lett. B562 (2003) 182, hep-ex/0212039.
- [60] B.Q. Ma, I. Schmidt and J.J. Yang, Phys. Rev. D63 (2001) 037501, hep-ph/0009297.
- [61] B.Q. Ma, I. Schmidt and J.J. Yang, Phys. Rev. D65 (2002) 034010, hep-ph/0110324.
- [62] Belle, K. Abe et al., Phys. Rev. Lett. 96 (2006) 232002, hep-ex/0507063.
- [63] Belle, A. Ogawa et al., AIP Conf. Proc. 915 (2007) 575.
- [64] Belle, R. Seidl et al., Phys. Rev. D78 (2008) 032011, 0805.2975.

- [65] S.J. Brodsky and S.D. Drell, Phys. Rev. D22 (1980) 2236.
- [66] S.J. Brodsky, M. Burkardt and I. Schmidt, Nucl. Phys. B441 (1995) 197, hep-ph/9401328.
- [67] M. Gockeler et al., Nucl. Phys. Proc. Suppl. 153 (2006) 146, hep-lat/0512011.
- [68] D. Boer et al., (2011), in preparation.
- [69] A. Idilbi et al., Phys. Rev. D70 (2004) 074021, hep-ph/0406302.
- [70] Jefferson Lab Hall B, S. Kuhn et al., PAC30 Proposal (2006).
- [71] H. Avakian and P. Bosted., (2006).
- [72] L. Mankiewicz, A. Schafer and M. Veltri, Comput. Phys. Commun. 71 (1992) 305.
- [73] A.V. Efremov, K. Goeke and P. Schweitzer, Czech. J. Phys. 55 (2005) A189, hep-ph/0412420.
- [74] K. Goeke et al., Phys. Lett. B567 (2003) 27, hep-ph/0302028.
- [75] J.P. Chen et al., JLab Experiment E12-11-007 (2008).
- [76] Jefferson Lab Hall B, . H.Avakian et al., LOI to PAC30 (2006).